Available online at www.sciencedirect.com
SCIENCE DIRECT®
Carbon 43 (2005) 2579–2587
CARBON
www.elsevier.com/locate/carbon

Polyaniline-carbon composite films as supports of Pt and PtRu particles for methanol electrooxidation

Gang Wu *, Li Li, Jing-Hong Li, Bo-Qing Xu *

Innovative Catalysis Program, Key Laboratory of Organic Optoelectronics and Molecular Engineering, Department of Chemistry, Tsinghua University, Beijing 100084, China

Received 3 December 2004; accepted 10 May 2005
Available online 24 June 2005

Abstract

Vulcan XC-72 carbon black particles (average size: ca. 50 nm) was incorporated into polyaniline (PANI) matrix by an electrochemical codeposition technique during the electropolymerization process. The doping by carbon particles leads to a higher polymeric degree and a lower defect density in the PANI structure. Furthermore, the incorporation of carbon particles not only increases the electrochemical accessible surface areas (S_a) and electron conductivity of the PANI film, but also decreases charge transfer resistance at PANI/electrolyte interfaces. Therefore, as expected, a fabricated PANI + C composite film with dispersed Pt and PtRu particles exhibited excellent electrocatalytic activity for methanol oxidation due to better Pt dispersion and utilization. The PANI + C composite film is more promising as a support material in electrocatalysis than a PANI film. Meanwhile, a new application for regular carbon black as a doping material into conducting polymer for electrocatalysis was thus demonstrated.

Keywords: Carbon black; Catalyst support; Photoelectron spectroscopy; Catalytic properties; Electrochemical properties

1. Introduction

Carbon materials have been generally used to support nano-sized Pt and Pt based particles for the electrocatalytic oxidation of methanol in direct methanol fuel cells (DMFCs) [1–3]. At present, one of the premier carbon supports is Vulcan XC-72 carbon black. However, the low rate of methanol electrooxidation is partly due to low utilization of Pt in this conventional carbon (XC-72) supported catalyst, owing to low electrochemical accessible surface area for the deposition of Pt particles [4]. Moreover, XC-72 carbon particles generally contain sulfur groups and may cause Pt particle aggregation [5].

Therefore, considerable efforts have been devoted to the optimization and development of new carbon support materials to improve both the oxidation rate and electrode stability for methanol electrooxidation, such as graphite nanofibers (GNFs) [6], carbon nanotubes (CNTs) [7] and mesocarbon microbeads (MCMB) [8] providing new candidate carbon supports for Pt and Pt-based electrocatalysts. On the other hand, electron conducting polymers such as polyaniline (PANI), as a new form of support for electrocatalysts involving the electrooxidation of small molecules, have received much attention because of their high accessible surface area, low resistance and high stability [9]. Consequently, dispersing metal particles into PANI films during or after the polymerization process is an attractive method to prepare electrocatalysts [10,11]. It had been confirmed from Auger electron spectroscopy (AES) [12] and cross-sectional SEM imaging [13] that metal particles

* Corresponding authors. Tel.: +86 10 62795834; fax: +86 10 62792122.
E-mail addresses: wugang@tsinghua.edu.cn (G. Wu), bqxu@tsinghua.edu.cn (B.-Q. Xu).

0008-6223/$ - see front matter © 2005 Elsevier Ltd. All rights reserved.
doi:10.1016/j.carbon.2005.05.011

can be three-dimensionally homogeneously dispersed into a porous PANI film by a constant potential electrodeposition technique. The well-dispersed Pt particles inside such conducting polymer supports can lead to better Pt utilization and an improvement of the catalytic mass activity for the methanol oxidation. Moreover, the interaction of the deposited Pt particles with the conducting polymer matrix would favor the formation of OH species at a low positive potential thus increasing the reaction rate of methanol oxidation [14]. However, despite what a conducting PANI film can offer as a support material in electrocatalysis, some disadvantages still limit its application, for example, loose and porous fibrous morphology, long polymerization time and insufficient electron conductivity [15,16].

To improve the properties of PANI for various applications such as light-emitting diodes, chromatography, electrostatic discharge protection and corrosion-protecting paint, some new attempts have been made to design and synthesize PANI/carbon nanotube composite materials by chemical routes [17–19]. However, to the best of our knowledge, there have been no reports either on the synthesis of conducting polymer/carbon particle composite film by the electrochemical codeposition technique or its use as a support material in electrocatalysis. Here, considering the advantageous combination of conventional carbon support (XC-72) and conducting polymer materials (PANI), we demonstrate for the first time that nano-sized carbon black particles (XC-72) can be incorporated into the PANI matrix by electrochemical codeposition during the process of electropolymerization to fabricate composite materials used for support materials in electrocatalysis. Furthermore, Pt and PtRu particles were dispersed in the PANI + C composite film by constant potential electrodeposition and show much higher electrochemical activity for methanol oxidation. In addition, utilization of Vulcan XC-72 for doping polymers to be used in electrocatalysis demonstrates a new application for regular carbon black products.

2. Experimental

2.1. Features of carbon black particles (Vulcan XC-72)

The features of the Vulcan XC-72 carbon black particles (Cabot International) used for doping the polymer were characterized by various techniques. Surface morphology was examined using a Hitachi S-5400 scanning electron microscope (SEM). High-resolution transmission electron microscopy (HRTEM) was conducted on a Hitachi H-9000 300 kV microscope. Crystallinity was evaluated by X-ray diffraction (XRD) performed on a Bruker d8 diffractometer system equipped with a Cu Kα radiation and a graphite monochromator operated at 45 kV and 40 mA. Specific surface area and porous size distribution were also investigated by Brunauer–Emmett–Teller (BET) analyses with nitrogen adsorption–desorption isotherms on a Micromeritics ASAP 2010 C instrument at 77 K.

2.2. Synthesis of PANI + C composite film

A glassy carbon (GC) rotating disc electrode (RDE) was used as a substrate for the PANI or PANI + C film. Freshly distilled aniline was used to prepare a solution of 0.1 M $C_6H_5NH_2$ + 0.5 M H_2SO_4. The Vulcan XC-72 carbon black particles were added in the above solution at a concentration of 1 g/l. To fabricate PANI and PANI + C film, a GC rotating disc as a working electrode was subjected to a cyclic potential ranging from 0 V to 1.1 V at a 50 mV/s sweep rate in the above aniline solutions with and without suspended carbon particles. The thickness of the PANI and PANI + C films was determined by the total anodic charge, supposing that a charge of 16 mC/cm^2 corresponds to a thickness of 0.063 μm [20]. Surface morphology of electropolymerized PANI and PANI + C films were also examined using the SEM.

2.3. Physical and electrochemical characterizations of PANI + C film

The polymeric structure and surface state of the PANI and PANI + C films were determined by XPS using an ESCA 210 and MICROLAB 310 D spectrometer.

The PANI and PANI + C films deposited on the GC RDE were characterized by cyclic voltammograms (CV) and electrochemical impedance spectroscopy (EIS) in 0.5 M H_2SO_4. The sweep rate in CV measurements was 20 mV/s. EIS measurements were performed under open circuit potential between 100 kHz and 0.1 Hz with an excitation signal of 5 mV. To analyze their impedance parameters, the impedance spectra were fitted by the Zsimpwin program.

2.4. Methanol electrooxidation on Pt and PtRu dispersed into PANI + C film

To investigate methanol electrooxidation on PANI and PANI + C films with dispersed Pt and PtRu particles, electrodeposition of Pt and PtRu particles into PANI or PANI + C composite films was conducted. Electrodeposition of Pt was performed in 0.5 M H_2SO_4 + 3 mM H_2PtCl_6 solution at constant potential 0.05 V for different times to obtain various Pt loadings. For the PtRu particles, the electrodeposition was carried out in 0.5 M H_2SO_4 solution containing x mM H_2PtCl_6 + $(3 - x)$ mM $RuCl_2$ ($x = 2, 1.5, 1$) at constant potential of −0.1 V. The Pt and Ru contents were determined by energy dispersion spectroscopy (EDS).

Electrocatalytic oxidation of methanol was examined in 0.5 M CH_3OH + 0.5 M H_2SO_4 solutions by the CV technique at 20 mV/s between 0 V and 0.95 V. In this work, an EG&G model 273 potentiostat/galvanostat and 1025 frequency response were used for all electrochemical measurements in a conventional three-electrode cell, using a saturated calomel electrode (SCE) as reference electrode and a large-area Pt sheet as counter electrode at room temperature (23 ± 2 °C).

3. Results and discussion

3.1. Features of carbon particles (Vulcan XC-72)

Fig. 1 shows SEM and HRTEM micrographs of carbon black particles (Vulcan XC-72). The material is made of somewhat spherical aggregates about 100–200 nm in size (Fig. 1a), each aggregate being made of elementary particles about 50 nm (Fig. 1b).

Fig. 1c shows the XRD pattern of XC-72 carbon black particles. The carbon particles exhibit obvious polyaromatic, turbostatic structural features with 002 and 10 peaks, despite the fact that some amorphous structures may coexist due to the large half-peak width and low intensity of the related 002 reflection. The fact that the 004 peak is nearly absent relates to the poor crystallinity of the material, and specifically to the low average number of graphenes stacked within the coherent domains. Since it has been reported [21] that graphitic crystallinity is important for electron transport during the electrochemical reaction because of the good electron conductivity of graphite and its interaction with loaded metal particles, it was interesting to see whether a carbon black grade with such a low degree of graphitization as Vulcan XC-72 would improve the usefulness of PANI films in support materials applications.

The carbon black particles were also evaluated from BET analyses. The BET specific surface area of the carbon sample is about 216 m^2/g. Meanwhile, the pore diameter distribution is shown in Fig. 1d and shows that the dominant pore diameter of the carbon particles is about 2–10 nm, which is in the mesopore range. In fact, a mesoporous structure is a key factor contributing to the feasibility of carbon supports in electrocatalysis [22].

3.2. Electropolymerization of PANI + C films

In order to compare the electropolymerization process between PANI and PANI + C composite film, cyclic voltammograms (CV) for 1st, 20th and 30th cycles were recorded and shown in Fig. 2. As can be seen in Fig. 2a, the electropolymerization of aniline starts at 0.85 V in the first cycle and shows a ''nucleation-loop'' due to aniline monomer oxidation and film formation [23]. Subsequent cycles indicate that three pairs of redox peaks labeled A/A′–C/C′ are observable. Peaks A–C correspond to the formation of radical cations (peak A, 0.40 V), oxidation of head-to-tail dimer (peak B, 0.68) and conversion from emeraldine to pernigraniline structures (peak C, 0.95 V), respectively [24]. From a comparison of Fig. 2a and b, despite the similar

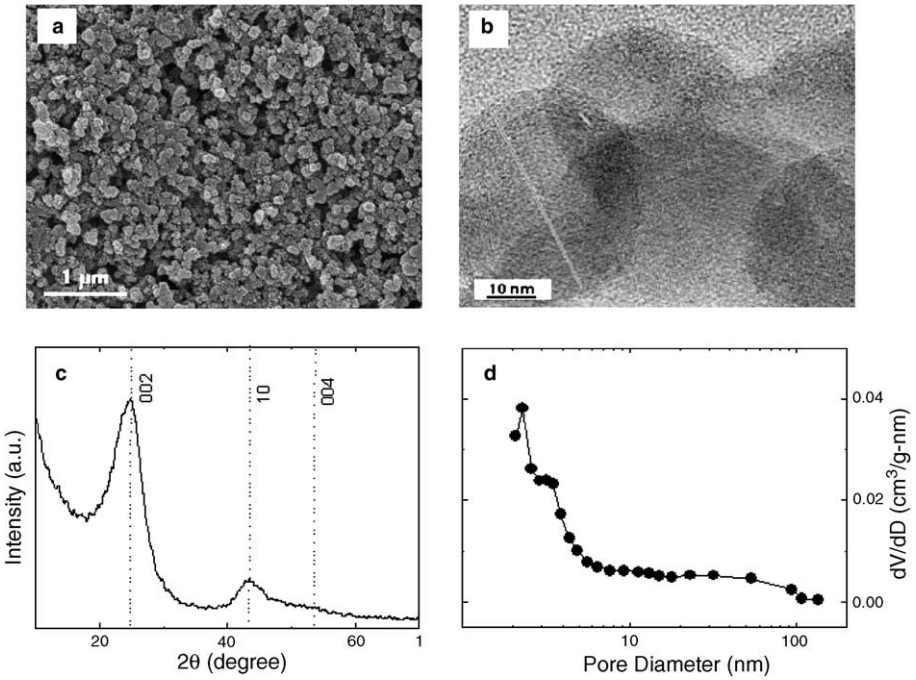

Fig. 1. (a) SEM image, (b) high-resolution TEM image, (c) XRD pattern and (d) pore size distribution of the carbon black particles (Vulcan XC-72).

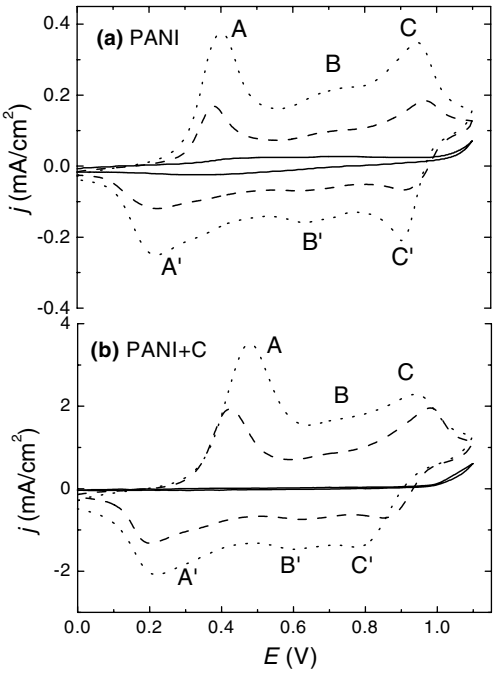

Fig. 2. Electropolymerization process of PANI (a) and PANI + C (b) at 1st (—), 20th (– – –) and 30th (. . .) cycles.

polymerization behaviors for PANI and PANI + C films, indicating that the mechanism of aniline polymerization is not significantly affected by the presence of carbon particles. It should be noted that the current of peak C on the 30th cycle for PANI + C is almost six times higher than that for PANI. This reveals that the electropolymerization rate of aniline is undoubtedly accelerated by the incorporation of carbon particles. This may be because the carbon particle is a good electron acceptor and aniline is a fairly good electron donor. Therefore, this complex with strong interactions leads to charge stabilization and thus effectively promotes the polymerization of PANI [25].

The morphology of PANI and PANI + C films synthesized by CV is shown in Fig. 3. PANI film (Fig. 3a) exhibits a nanofibrous surface structure and the fiber has a diameter of 100–200 nm and a length of about 1–2 μm. Compared with the PANI film, the incorporated spherical aggregated carbon particles can be detected with a size scale of 100–200 nm in the PANI + C composite film. The latter exhibits a more compact aspect and has relatively smaller pores, and the close contact between the carbon particles and the polymer is expected to increase the conductivity of the polymer.

3.3. XPS analysis of PANI + C films

The electrochemical reversibility, stability and conductivity of PANI may be linked to the intrinsic structure of conducting polymers. Hence, PANI and PANI + C films were subjected to the XPS examination to investigate the effect of incorporated carbon particles on the intrinsic structure of the polyaniline matrix. As expected, the relative concentrations of elemental C in the PANI + C composite film are obviously higher (69.1%) than that in the PANI film (60.1%). Furthermore, in order to speculate on the influence of incorporated carbon particles on the intrinsic oxidation state and protonation level of PANI structures, N 1s and C 1s core-levels can be quantitatively deconvoluted.

Typical XPS N 1s core-level spectra for the PANI and PANI + C composite films are shown in Fig. 4. These spectra show relatively broad peaks, suggesting the existence of several structures. Thus, the XPS peaks of N 1s are reasonably composed of four Gaussian–Lorentzian peaks with the binding energy of approximate 398.7, 399.8, 401.6 and 402.8 eV. The peak with the lowest binding energy (398.7 eV) is due to the imine-like (=N–) structure, and the peak centered at 399.8 eV is attributed to the amine-like nitrogen atoms (–NH–) [26]. The peak centered at 401.6 eV is attributed to the cationic nitrogen atoms on the polymer backbone compensated with the counterions (SO_4^{2-}) and the highest binding energy (402.8 eV) peak is due to the protonated amine units [27]. The ratio of [=N–]/[–NH–] provides a direct evaluation of the intrinsic oxidation state of PANI and is indicative of the polymeric level [28]. Therefore, the value of [=N–]/[–NH–] for

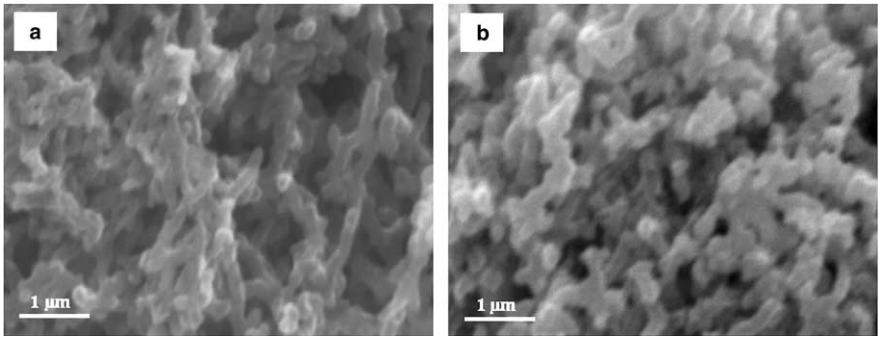

Fig. 3. SEM images of (a) PANI, (b) PANI + C composite film.

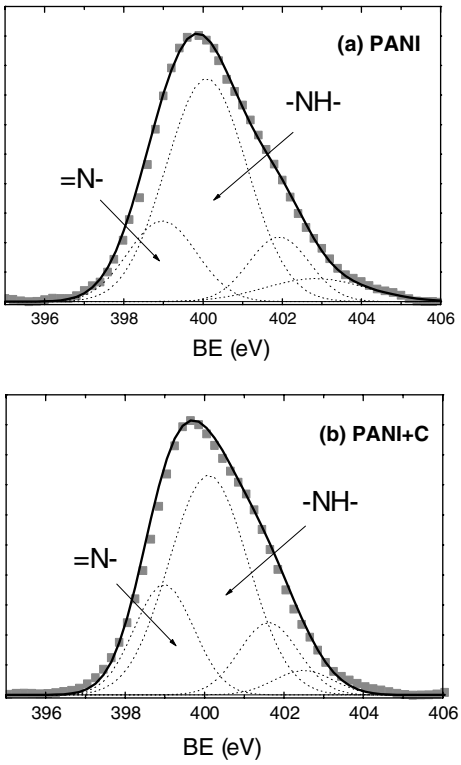

Fig. 4. XPS spectra of N 1s for (a) PANI and (b) PANI + C composite film.

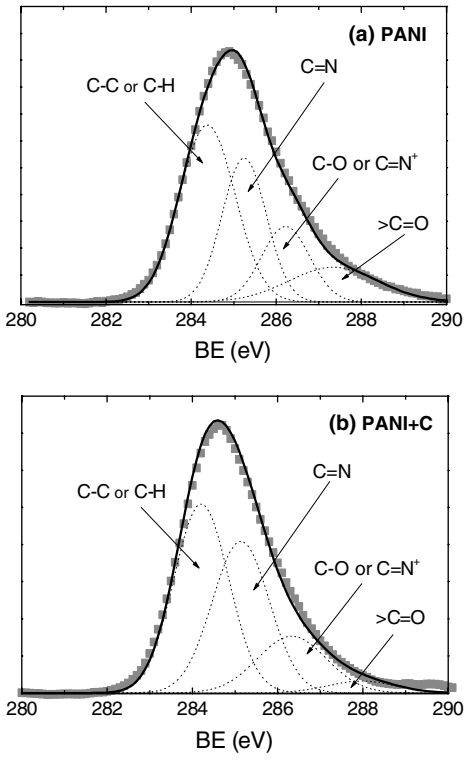

Fig. 5. XPS spectra of C 1s for (a) PANI and (b) PANI + C composite film.

PANI + C film (0.38) is obviously higher than that of PANI (0.30) suggesting that the intrinsic oxidation state of the PANI + C is increased with the incorporation of carbon particles.

The XPS C 1s core-level spectra for the PANI and PANI + C films are shown in Fig. 5. All these C 1s spectra show asymmetric characteristics, indicating the presence of structure defects [29]. Through Gaussian–Lorentzian fitting, these C 1s spectra can be separated into four peaks, centered at about 284.1 (C–C or C–H), 285.1 (C═N), 286.1 (C═N^+ or –C–O) and 287.9 eV (>C═O), [30]. In particular, the relative areas of the two higher binding-energy peaks (286.1 and 287.9 eV) are used to calculate the density of carbonyl defects within polymers, showing the degradation of the polymer [31]. Therefore, the values of the relative areas in the PANI + C composite film (19%) is lower than that of the PANI film (32%) indicating a low defect density due to the incorporation of carbon particles.

As a result, the XPS analyses show that the PANI film doped with carbon particles has a higher polymeric degree and a lower defect density, which probably results in better electrochemical properties and electron conductivity. With these premises, we carried out the following experiments to investigate the effect of the incorporated carbon particles on the electrochemical performance of the PANI film.

3.4. Electrochemical characterization of PANI + C films

Fig. 6 compares the CVs of the PANI and PANI + C films in 0.5 M H_2SO_4 solution. In general, the electrochemical accessible surface area S_a (m^2/g) is dependant on the gravimetric double layer capacitance C (F/g) and can be calculated from the currents at a chosen potential (0.55 V) in the CV curves. Thus, according to the related equations [32], the S_a for PANI + C composite film is 550.0 m^2/g and obviously higher than that of PANI (257.5 m^2/g).

Impedance spectra of the conducting polymer can be considered to study film conductivity, structures and

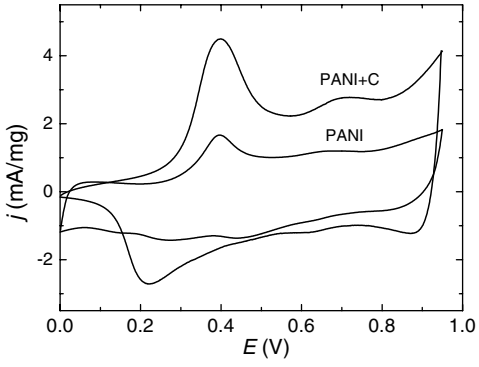

Fig. 6. Cyclic voltammograms of PANI and PANI + C films in 0.5 M H_2SO_4 solution at a sweep rate of 20 mV/s.

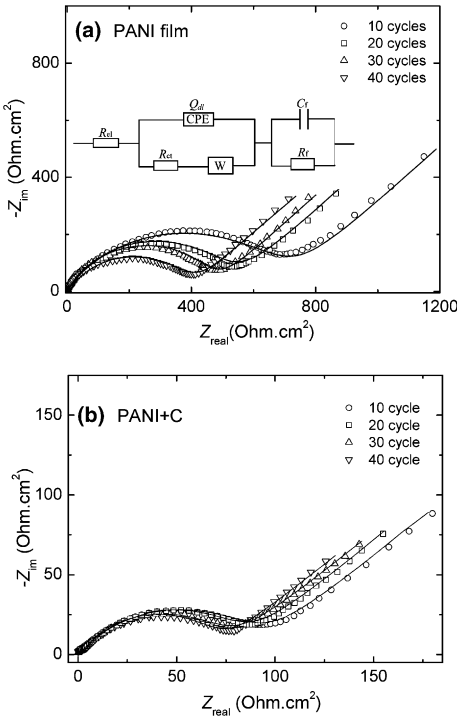

Fig. 7. Nyquist plots of PANI (a) and PANI + C (b) after different electropolymerization cyclic numbers. Points are experimental data and solid lines are fitted curves. Inset is equivalent circuit for PANI and PANI + C film in H_2SO_4 solution: R_{el} solution resistance; R_{ct} charge transfer resistance; Q_{dl} constant phase element related to double layer capacitance; W Warburg impedance; R_f film resistance; C_f film capacitance.

charge transport in polymer film/electrolyte interface. Therefore, the Nyquist plots for PANI and PANI + C films at different cycle numbers in electropolymerization are shown in Fig. 7a and b, respectively. According to the impedance spectra of polymer film coated on metals in the asymmetric metal/film/electrolyte configuration [11,33], an equivalent circuit inserted in Fig. 7a can be used to represent the impedance behavior of PANI and PANI + C composite films in H_2SO_4 solution at open circuit potential. The good fits (solid lines in Fig. 7) imply that the equivalent circuit models can reasonably explain the electrochemical processes occurring in PANI and PANI + C films. Furthermore, according to the equivalent circuit, the simulated values of the impedance parameters can be determined by a complex nonlinear least squares (CNLLS) fitting procedure and are listed in Table 1. By comparing the fitted results, a greater constant phase element (CPE) representing double layer capacitance and smaller charge transfer resistance (R_{ct}) are found for PANI + C composite films, suggesting a higher S_a and easier charger transfer at the interface (polymer/electrolyte). Moreover, the film resistance R_f is also found to decrease from 14.0 Ω cm^2 for PANI to 3.4 Ω cm^2 for PANI + C composite film after 40 cycles electropolymerization.

Therefore, it is clear from above results that the incorporation of carbon particles into the PANI matrix lead to a larger S_a for the film and an easier charge transfer at the polymer/electrolyte interface as well as a higher conductivity of the polymer film. All have a positive effect on the electrochemical properties of PANI films.

3.5. Methanol oxidation on Pt–PANI and Pt–PANI + C catalyst

To evaluate the performance of PANI and PANI + C films as support materials in the electrooxidation of methanol, various Pt loadings (0–80 μg/cm^2) were electrodeposited on both films. CV curves for methanol oxidation on Pt–PANI and Pt–PANI + C are shown in Fig. 8a and b, respectively. All the current density values are expressed taking into account of geometric area, representing mass activity of electrocatalyst. Obviously, compared to Pt–PANI, larger peak currents of methanol oxidation were obtained on Pt–PANI + C. Especially, at a Pt loading of 80 μg/cm^2, Pt–PANI + C exhibits about a four times higher peak current (i.e. mass activity) than that of the Pt–PANI catalyst. Furthermore, it should be noticed that the linear relationship (inset of Fig. 8) between the peak currents and increased Pt loading can be detected, supporting the assumption that an increased Pt deposition amount (0–80 μg/cm^2) results in an increase in the number of Pt particles and not a significant increase in size of the particles.

According to previous results from CV and EIS characterization, it is maybe reasonable that the better mass activity on Pt–PANI + C is due to higher Pt dispersion

Table 1
Fitted impedance parameters for PANI and PANI + C films in 0.5 M H_2SO_4 solution at open circuit potential

Film	Cycle number	CPE × 10^5 (Ω^{-1} s^n cm^{-2})	n	R_{ct} (Ω cm^2)	W × 10^3 (Ω^{-1} cm^{-2} s$^{0.5}$)	C_f × 10^6 (F cm^{-2})	R_f (Ω cm^2)
PANI	10	0.3	0.81	657	0.7	0.1	6.9
	20	0.5	0.76	512	1.8	0.9	6.8
	30	1.3	0.74	438	2.0	2.8	10.7
	40	1.7	0.71	375	3.1	3.9	14.0
PANI + C	10	5.4	0.79	87.1	7.7	1.2	2.1
	20	6.1	0.74	80.9	9.5	2.3	2.6
	30	8.9	0.73	73.7	10.4	5.8	2.7
	40	10.1	0.71	71.2	10.9	16.2	3.4

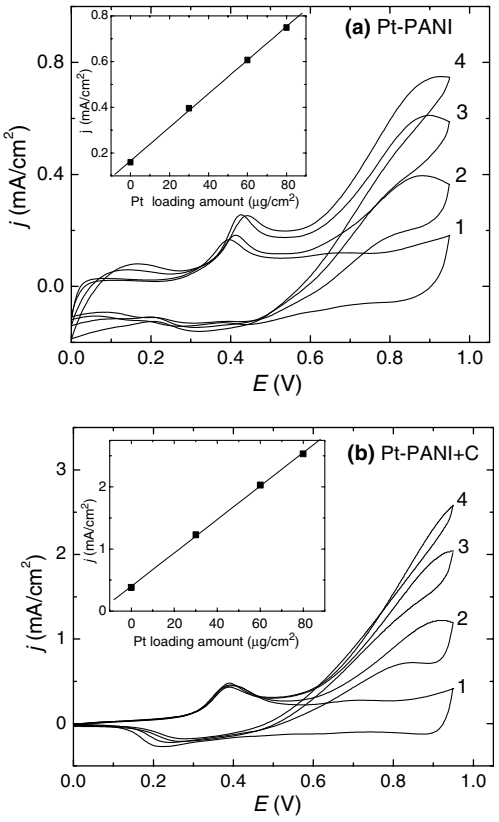

Fig. 8. Methanol electrooxidation on (a) Pt–PANI and (b) Pt–PANI + C catalysts with various Pt loadings (1) 0, (2) 30, (3) 60, (4) 80 μg/cm^2.

and utilization, which can be attributed to the higher accessible electrochemical areas (S_a) of the composite films. In addition, high conductivity (ionic and electronic) of the PANI + C composite film also helps achieve a high mass activity for methanol oxidation.

3.6. Methanol oxidation on PtRu–PANI + C catalyst

In order to optimize the contents of electrodeposited PtRu particles dispersed into the PANI + C composite films for methanol oxidation, solutions with various Pt:Ru atomic ratios (1:2, 1:1, 2:1) were chosen. The metal loading was controlled at 100 μg/cm^2. The CV curves of methanol oxidation on the three PtRu–PANI + C samples are shown in Fig. 9. Two key parameters used to evaluate electrocatalytic activity are onset potential and peak current of methanol electrooxidation [34]. The results indicate that the PtRu particles electrodeposited from a Pt:Ru = 2:1 atomic ratio solution corresponding to a Ru content of 14 at.%, exhibit the highest electrocatalytic activity i.e. the lowest onset potential (0.35 V) and the highest peak current (5.8 mA/cm^2). Gasteiger and co-workers [35] also reported similar results that the sputter-cleaned polycrystalline PtRu alloy with a surface of about 10 at.% Ru, had the highest catalytic activity toward the electrooxidation of methanol. So, the combination of optimal PtRu particles with excellent catalytic activity and PANI + C composite support with high electrochemical accessible surface areas and conductivity can become a promising electrocatalyst for methanol oxidation in DMFCs.

4. Conclusion

Vulcan XC-72 carbon particles, which were used for electrochemical codeposition into a conducting polymer during electropolymerization, were characterized by SEM, HRTEM, XRD and BET. The composite conducting polymer film (PANI + C) can serve as a support material for dispersing Pt and PtRu particles in an electrocatalyst for methanol oxidation. The incorporation of carbon particles may play an important role for the improvement of the physical and electrochemical properties of the PANI film. Likewise, the PANI film also provides a suitable matrix for conventional carbon black particles and forms composite support materials with increased electrochemical accessible surface area and decreased charge transfer resistance.

Electrochemical characterizations of PANI and PANI + C films fabricated in our experimental conditions show that the doping of carbon particles into

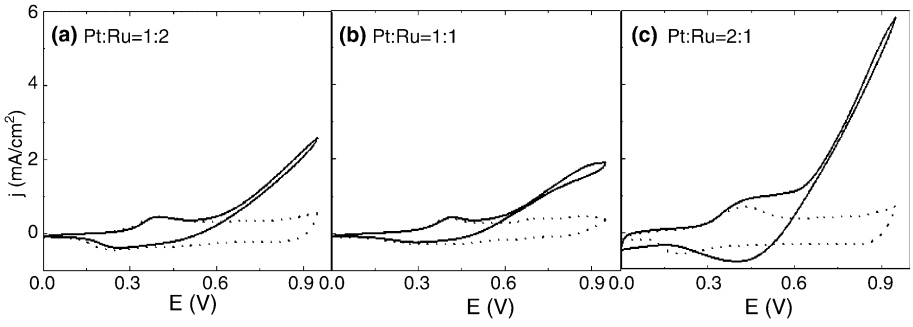

Fig. 9. Methanol electrooxidation on PtRu particles deposited into the PANI + C composite film from different Pt:Ru atomic ratio solutions (a) Pt:Ru = 1:2, (b) Pt:Ru = 1:1, (c) Pt:Ru = 2:1 with same metal loading, 100 μg/cm^2, in 0.5 M H_2SO_4 (. . .) and 0.5 M H_2SO_4 + 0.5 M CH_3OH solutions (—).

PANI films causes S_a to increase from 257.5 m^2/g for PANI to 550.0 m^2/g for PANI + C composite films, the film resistance R_f decreasing from 14.0 $\Omega\,cm^2$ to 3.4 $\Omega\,cm^2$ and the charge transfer resistance R_{ct} at polymer/electrolyte interfaces also decreases from 375 $\Omega\,cm^2$ to 71.2 $\Omega\,cm^2$ in 0.5 M H_2SO_4 solution at open circuit potential. As expected, Pt–PANI + C exhibits about a four times higher mass activity for methanol oxidation in comparison with Pt–PANI at a Pt loading of 80 μg/cm^2. However, it should be stressed that the improvement caused by the doping of carbon particles is dependent on the amount of carbon particles incorporated which is determined by both the carbon particle concentration in the electrolytes and the hydrodynamic conditions in electrochemical codeposition. Future work will focus on these issues. In addition, we also consider highly graphitized carbon black or other carbon materials such as carbon nanotubes exhibiting a higher electron conductivity than Vulcan XC-72 to act as doping material and to evaluate how much the performance of the composite can be further improved.

Finally, the data of the present study suggest that the optimal PtRu particles banding with the excellent PANI + C composite film would be a promising electrocatalyst for potential application in methanol electrooxidation. This work also demonstrated a new application for conventional carbon black particles such as Vulcan XC-72 as doping materials in a conducting polymer to be used as catalyst support in the electrooxidation processes.

Acknowledgements

The authors wish to acknowledge the financial support of this work from Ministry of Science and Technology of China (Grant: G2000026408), NSF (Grant: 20125310) and China Postdoctoral Science Foundation (2004035300).

References

[1] Batista EA, Malpass GRP, Motheo AJ, Iwasita T. New insight into the pathways of methanol oxidation. Electrochem Commun 2003;5(10):843–6.
[2] Iwasita T. Electrocatalysis of methanol oxidation. Electrochim Acta 2002;47(22–23):3663–74.
[3] Valbuena WHL, Paganin VA, Leite CAP, Galembeck F, Gonzalez ER. Catalysts for DMFC: relation between morphology and electrochemical performance. Electrochim Acta 2003; 48(25–26): 3869–78.
[4] Shi H. Activated carbons and double layer capacitance. Electrochim Acta 1996;41(10):1633–9.
[5] Roy SC, Christensen PA, Hamnett A, Thomas KM, Trapp V. Direct methanol fuel cell cathodes with sulfur and nitrogen-based carbon functionality. J Electrochem Soc 1996;143(10):3073–9.
[6] Liu ZL, Lin XH, Lee JY, Zhang W, Han M, Gan LM. Preparation and characterization of platinum-based electrocatalysts on multi-walled carbon nanotubes for proton exchange membrane fuel cells. Langmuir 2002;18(10):4054–60.
[7] Li WZ, Liang CH, Zhou WJ, Qiu JS, Zhou ZH, Sun GQ, et al. Preparation and characterization of multiwalled carbon nanotube-supported platinum for cathode catalysts of direct methanol fuel cells. J Phys Chem B 2003;107(26):6292–9.
[8] Liu YC, Qiu XP, Huang YQ, Zhu WT. Methanol electrooxidation on mesocarbon microbead supported Pt catalysts. Carbon 2002;40(13):2375–80.
[9] Inzelt G, Pineri M, Schultze JW, Vorotyntsev MA. Electron and proton conducting polymers: recent developments and prospects. Electrochim Acta 2000;45(15–16):2403–21.
[10] Rajesh B, Thampi KR, Bonard JM, McEvoy AJ, Xanthopoulos N, Mathieu HJ, et al. Pt particles supported on conducting polymeric nanocones as electro-catalysts for methanol oxidation. J Power Sources 2004;133(2):155–61.
[11] Niu L, Li QH, Wei FH, Chen X, Wang H. Electrochemical impedance and morphological characterization of platinum-modified polyaniline film electrodes and their electrocatalytic activity for methanol oxidation. J Electroanal Chem 2003;544(6):121–8.
[12] Lai EKW, Beattie PD, Orfino FP, Simon E, Holdcroft S. Electrochemical oxygen reduction at composite films of Nafion, polyaniline and Pt. Electrochim Acta 1999;44(15):2559–69.
[13] Kost KM, Bartak DE, Kazee B, Kuwana T. Electrodeposition of platinum microparticles into polyaniline films with electrocatalytic applications. Anal Chem 1988;60(21):2379–84.
[14] Frelink T, Visscher W, Veen JAR. Particle-size effect of carbon-supported platinum catalysts for the electrooxidation of methanol. J Electroanal Chem 1995;382(1–2):65–72.
[15] Inzelt G, Csahok E, Kertesz V. Preparation and characterization of polyaniline electrode modified with diamino-methylbenzoate. Electrochim Acta 2001;46(26–27):3955–62.
[16] Zhang QH, Wang XH, Chen DJ, Jing XB. Dynamic mechanical properties of melt processable PANI-DBSA/LDPE blends. Synth Met 2003;135(1–3):481–2.
[17] Wu TM, Lin YW, Liao CS. Preparation and characterization of polyaniline/multi-walled carbon nanotube composites. Carbon 2005;43(4):734–40.
[18] Zhang XT, Zhang J, Wang RM, Liu ZF. Cationic surfactant directed polyaniline/CNT nanocables: synthesis, characterization, and enhanced electrical properties. Carbon 2004;42(8–9): 1455–61.
[19] Li XH, Wu B, Huang JE, Zhang J, Liu ZF, Li HL. Fabrication and characterization of well-dispersed single-walled carbon nanotube/polyaniline composites. Carbon 2003;41(8):1670–3.
[20] Stilwell DE, Park SM. Electrochemistry of conductive polymers III: some physical and electrochemical properties observed from electrochemical grown polyaniline. J Electrochem Soc 1988;135(10):2491–6.
[21] Park KW, Sung YE, Han S, Yun Y, Hyeon T. Origin of the enhanced catalytic activity of carbon nanocoil-supported PtRu alloy electrocatalysts. J Phys Chem B 2004;108(3):939–44.
[22] Pietron JJ, Stroud RM, Rolison DR. Using three dimensions in catalytic mesoporous nanoarchitectures. Nano Lett 2002;2(5):545–9.
[23] Shim YB, Won MS, Park SM. Electrochemistry of conductive polymers VIII. In situ spectroelectrochemical studies of polyaniline growth mechanisms. J Electrochem Soc 1990;137(2): 538–43.
[24] Rapta P, Lukkari J, Tarabek J, Salomaki M, Jussila M, Yohannes G, et al. Ultrathin polyelectrolyte multilayers: in situ ESR/UV–Vis–NIR spectroelectrochemical study of charge carriers formed under oxidation. Phys Chem Chem Phys 2004;6(2):434–41.
[25] Sun Y, Wilson SR, Schuster DI. High dissolution and strong light emission of carbon nanotubes in aromatic amine solvents. J Am Chem Soc 2001;123(22):5348–9.

[26] Zhou YK, He BL, Zhou WJ, Li HL. Preparation and Electrochemistry of SWNT/PANI composite films for electrochemical capacitors. J Electrochem Soc 2004;151(7):A1052–7.
[27] Tan KL, Tan BTG, Kang ET, Neoh KG. X-ray photoelectron spectroscopy studies for the chemical structure of polyaniline. Phys Rev B 1989;39(11):8070–3.
[28] Kang ET, Neoh KG, Tan KL. Polyaniline with high intrinsic oxidation state. Surf Interface Anal 1993;20(9):833–40.
[29] Kang ET, Neoh KG, Tan KL. Handbook of organic conductive molecules and polymers. New York: Wiley; 1997. p. 85–97.
[30] Ribo JM, Dicko A, Tura JM, Bloor D. Chemical structure of polypyrrole: X-ray photoelectron spectroscopy of polypyrrole with 5-yliden-3-pyriolin-2-ine end groups. Polymer 1991;32(4):728–32.
[31] Schottland P, Zong K, Gaupp CL, Thompson BC, Thomas CA, Giurgiu I, et al. Poly(3,4-alkylenedioxypyrrole)s: highly stable electronically conducting and electrochromic polymers. Macromolecules 2000;33(19):7051–61.
[32] Zhou YK, He BL, Zhou WJ, Huang J, Li XH, Wu B, et al. Electrochemical capacitance of well-coated single-walled carbon nanotube with polyaniline composites. Electrochim Acta 2004;49(2):257–62.
[33] Tarola A, Dini D, Salatelli E, Andreani F, Decker F. Electrochemical impedance spectroscopy of polyalkylterthiophenes. Electrochim Acta 1999;44(24):4189–93.
[34] Wu G, Li L, Xu BQ. Effect of electrochemical polarization of PtRu/C catalysts on methanol electrooxidation. Electrochim Acta 2004;50(1):1–10.
[35] Markovic NM, Gasteiger HA, Ross PN, Jiang XD, Villegas I, Weaver MJ. Electrooxidation mechanisms of methanol and formic acid on Pt–Ru alloy surfaces. Electrochim Acta 1995;40(1):91–8.